Carbohydrate Research, 172 (1988) 113–138
Elsevier Science Publishers B.V., Amsterdam – Printed in The Netherlands

STRUCTURE DETERMINATION OF *Cryptococcus neoformans* SEROTYPE A-VARIANT GLUCURONOXYLOMANNAN BY ^{13}C-N.M.R. SPECTROSCOPY

ROBERT CHERNIAK, RONALD G. JONES*,

Department of Chemistry and Laboratory for Microbial and Biochemical Sciences, Georgia State University, Atlanta, Georgia 30303 (U.S.A.)

AND ERROL REISS

Immunology Branch, Division of Mycotic Diseases, Centers for Disease Control, Public Health Service, U.S. Department of Health and Human Services, Atlanta, Georgia 30333 (U.S.A.)

Received September 9th, 1986; accepted for publication, in revised form, June 2nd, 1987)

ABSTRACT

A series of polysaccharides was derived by physical and chemical methods from an antigenic, *O*-acetyl-containing, glucuronoxylomannan (GXM), isolated from the growth medium of *Cryptococcus neoformans* (CDC B2550) serotype A-variant having composition ratios of Man:Xyl:GlcA:OAc = 10:4:3:6. ^{13}C-N.m.r. spectra of derivatives provided new structural evidence for GXM. Treatment of GXM with Li in ethylenediamine gave a xylomannan (XM, with Man:Xyl = 5:2). Smith degradation of XM gave a mannan (M). Ultrasonic treatment of GXM gave GXM-sonicated (GXMS). Treatment of GXM with 3-(3-dimethylaminopropyl)-1-ethylcarbodiimide·HCl and then with $NaBH_4$ gave reduced GXMS (RGXMS), or with aq. trifluoroacetic acid gave partially acid-hydrolyzed GXMS. Periodate oxidation of GXM and $NaBH_4$ reduction of the product gave a polyalcohol-mannan (PM). Treatment of GXMS, RGXMS, and PM with NH_4OH at pH 11 gave the respective *O*-deacetylated analogs. Comparison among the ^{13}C-n.m.r. spectra of GXM, the various derivatives, and reference monosaccharides allowed the following conclusions: M is (1→3)-α-D-mannopyranan; XM consists of the M backbone with 91% of the Xyl on nonadjacent Man residues as 2-*O*-β-D-Xyl*p* substituents and with 9% as 4-*O*-D-Xyl*p* substituents on other Man residues. GXM consists of the XM structure, but with non-D-xylosylated Man residues substituted with 2-*O*-β-D-Glc*p*A substituents and with 6-*O*-acetyl groups distributed approximately equally on Man residues that have other substituents and those that have none. The molecular mechanics program MM2 was used to estimate the relative energies of anomeric orientations of the typical glycosidic linkage in M. The results suggest that 6′-OH ----O-2 H-bonding is significant in the minimal-energy orientation of M, with $\phi = -36°$ and $\psi = 51°$, and that two other glycosidic orientations may be important in the 2-*O*- or 6-*O*-substituted derivatives of M.

*To whom correspondence should be addressed.

0008-6215/88/$03.50

INTRODUCTION

The capsular polysaccharide of *Cryptococcus neoformans* inhibits phagocytosis[1–4] and is considered to be a major virulence factor: wild-type strains of *C. neoformans* are lethal for mice, whereas acapsular mutants are not[5]. Purified high-molecular-weight polysaccharides[6–12] have been obtained from the four recognized serotypes[13], A through D, of *C. neoformans,* and from the newly defined A-D serotype[14]. These are related, nonidentical, *O*-acetylated polysaccharides composed of glucuronic acid, xylose, and manose[6–12]. Structural models based on chemical methods suggest that the polysaccharides are composed of a linear backbone of α-(1→3)-linked D-mannopyranosyl residues (Man*p*) with *O*-xylopyranosyl (Xyl*p*), *O*-glucopyranosyluronic acid (Glc*p*A), and *O*-acetyl substituents[6–12]. The polysaccharides from serotypes A, D[8,10–12], and A-D[14] have Glc*p*A and Xyl*p* substituents attached through glycosidic linkages to O-2 atoms of the mannan backbone, whereas those from serotypes B and C[6,7,9] are similarly substituted at O-4, as well as O-2, atoms of the mannan. The anomeric configurations of the backbone and the glycosyl substituents are based on results of chromium trioxide oxidation, enzymic digestion with β-D-glucosiduronase, and optical-rotation analysis of derived oligosaccharides[8]. For reviews, see Bhattacharjee *et al.*[15] and Reiss *et al.*[16].

The exact disposition of the side-chain residues along the mannan backbone has not been determined, because methylation analysis does not reveal these details nor permit differentiation among block, random, or strictly repeating structural sequences. Therefore, the previously published depictions of *C. neoformans* polysaccharides must be considered to be equally representative models. The purpose of the present study was to continue the detailed structure elucidation of these polymers through application of ^{13}C-n.m.r. spectroscopy[17]. Previously, the only application extant was to serotype A polysaccharide, which consists of a complex spectrum published with an interpretation extended only to location of some of the *O*-acetyl groups on O-6 atoms of the mannan[12]. We now report the results of a ^{13}C-n.m.r.-spectral study of a series of structurally related polysaccharides obtained by physical and chemical modifications of a native polysaccharide of *C. neoformans* serotype A-variant. The n.m.r. data provide new evidence for the detailed, structural specification of this native polysaccharide.

EXPERIMENTAL

^{13}C-N.m.r. spectroscopy. — The ^{13}C-n.m.r. spectra were recorded with a JEOL-GX270 n.m.r. spectrometer operated at 67.80 MHz and equipped with a 5-mm, ^{1}H–^{13}C dual probe. The spectra were recorded at 70° by using the pulsed, fast Fourier-transform method. The deuterium resonance of the solvent, a buffer (pD 7.2) of sodium phosphate in deuterium oxide or dimethyl-d_6 sulfoxide (Me_2 SO-d_6), served as internal lock. The spectra were 16.025 kHz wide, and were collected with 32-k data points and by use of a 45° pulse repeated at intervals of 2.02 s. Fourier

transformations were executed with a 0.77-Hz broadening factor and zero-filling. The resulting, digital resolution in the 64-k data point frequency domain spectrum was 245 mHz or 0.0036 p.p.m. Proton-decoupled spectra were determined by application of a 3-kHz noise band at 270.05 MHz with an offset frequency at 118.333 kHz. Chemical shifts of the polysaccharides in D_2O solutions were measured relative to external sodium 4,4-dimethyl-4-silapentane-1-sulfonate (DSS) taken as 0.00 p.p.m. In order to relate polysaccharide chemical-shifts to literature values, the ^{13}C-chemical shifts of a mixture of methyl α-D-mannopyranoside (80 mg), methyl β-D-xylopyranoside (100 mg), and 1,4-dioxane (7 mg) in dilute buffered D_2O (0.50 mL) were measured relative to internal DSS (30 mg) from 30 to 90° in 10° increments. Under these conditions, the 1,4-dioxane chemical shift was found to be essentially constant at 68.904 ±0.008 p.p.m. Chemical shifts of the polysaccharides in Me_2SO-d_6 solutions were measured relative to the solvent resonance of 39.60 p.p.m. Carbon–hydrogen coupling constants were determined with gated decoupling providing retention of the nuclear Overhauser effect (n.O.e.), or sometimes without any form of proton-decoupling. The typical n.m.r. sample contained 50 mg of polysaccharide in 0.5 mL of buffered, 99.8 atom% deuterium oxide (Aldrich Chemical Co).

Native and modified glucuronoxylomannans (Scheme 1, steps a through g, and related polysaccharide derivatives. — (*a*) O-*Acetylglucuronoxylomannan (GXM).* Extracellular polysaccharides were recovered from filtrates of 96-h cultures of *Cryptococcus neoformans* (CDC B2550) serotype A-variant grown on chemically defined medium as previously described[18]. The culture, *Cryptococcus neoformans* 371A, was received from Dr. K. J. Kwong-Chung, National Institutes of Health, in 1977, and has been maintained in lyophilized form. In 1982, the isolation of both A and D clones from the original NIH culture was reported[12]. The culture, maintained at the Centers for Disease Control as CDC B2550, was cloned when originally received from NIH, and periodically checked by immunofluorescence[19] to verify that it was serotype A. In 1985, the isolate was resubmitted to the NIH laboratory, where the serotype was confirmed as A. No D clones have been observed in this culture, but the monosaccharide ratios of CDC B2550 capsular polysaccharide are different from the ratios published by the NIH group for their typical A serotype and for the variants they reported within NIH-371A. Therefore, CDC B2550 is referred to as serotype A-variant. The major viscous GXM was separated from other heteropolysaccharides by selective precipitation with hexadecyltrimethylammonium bromide[18].

(*b*) *Xylomannan (XM) by specific removal of glucuronic acid*[20,21] *from GXM.* GXM (145 mg, dried over P_2O_5 at 65°) was dissolved in ethylenediamine (20 mL, dried over CaH_2); when the majority of the polysaccharide had disolved (30 min of stirring), small pieces of lithium metal were added until a blue color persisted, an inert atmosphere (a positive pressure of argon) being used to prevent quenching. The mixture was stirred for 1–2 h at 20° with occasional additions of Li, as needed, to preserve the blue color. The reaction was terminated by adding sufficient dry

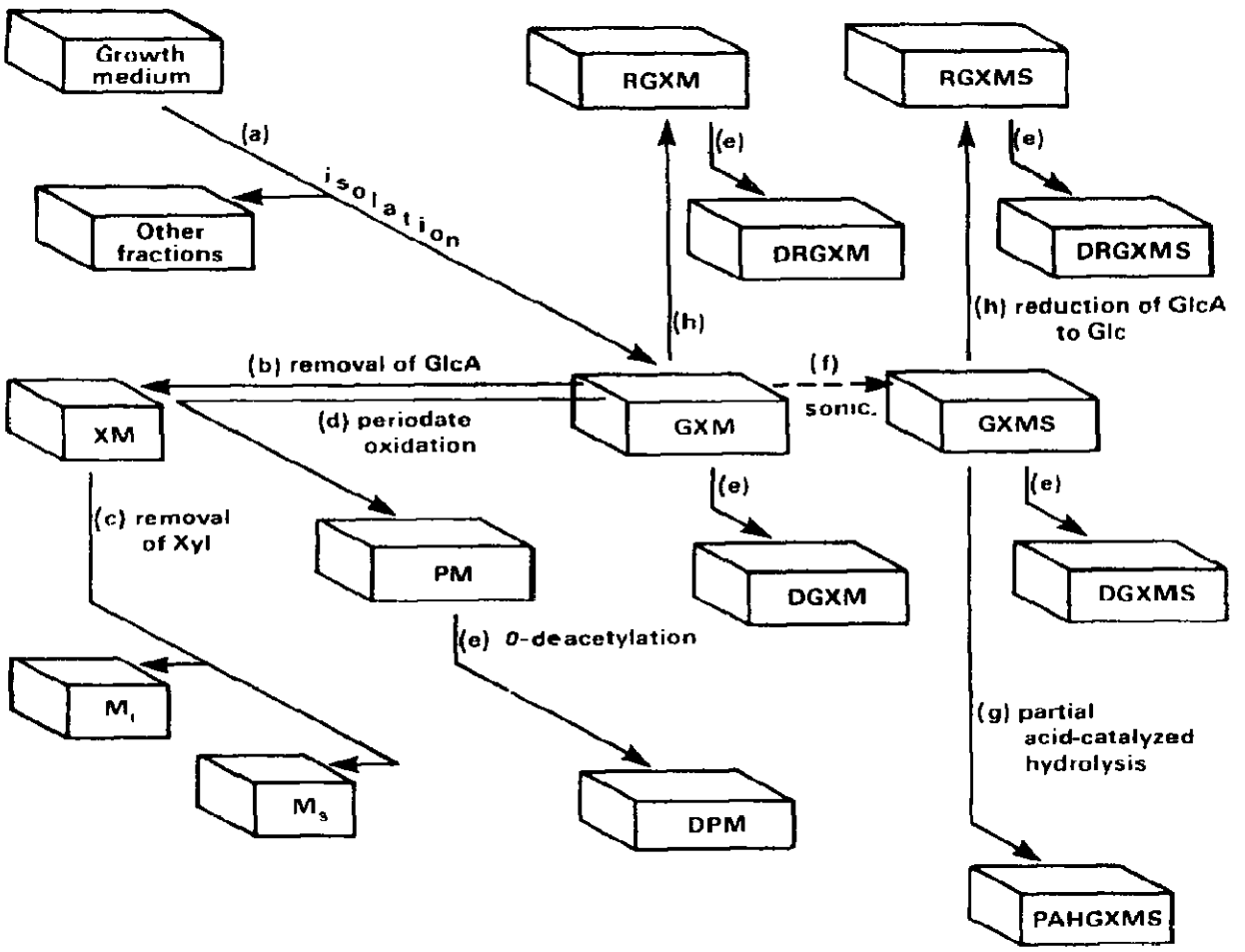

Scheme 1. Chemical derivation and relationships of polysaccharides prepared from the native *O*-acetylglucuronoxylomannan isolated from the growth medium of *Cryptococcus neoformans* serotype A-variant. The letters given with the arrows are keyed to lettered sections of the Experimental and Results sections, where appropriate literature references are provided. Definitions of acronyms: DGXM, *O*-deacetylated glucuronoxylomannan; DGXMS, *O*-deacetylated glucuronoxylomannan sonicated; DPM, *O*-deacetylated polyalcoholmannan; DRGXM, *O*-deacetylated reduced glucuronoxylomannan; DRGXMS, *O*-deacetylated reduced glucuronoxylomannan sonicated; GXM, native *O*-acetylglucuronoxylomannan; GXMS, *O*-acetylglucuronoxylomannan sonicated; M_i, mannan precipitated from aqueous solution; M_s, mannan recovered from supernatant aqueous solution; PAHGXMS, partial acid-catalyzed hydrolyzate from glucuronoxylomannan sonicated; RGXM, reduced glucuronoxylomannan; RGXMS, reduced glucuronoxylomannan sonicated; sonic., sonication; XM, xylomannan.

methanol to dispel the blue color, and the residual ethylenediamine was removed *in vacuo* over concentrated sulfuric acid. The yellow powder was dissolved in H_2O (20 mL), and the pH was immediately adjusted to 7 with concentrated HCl. The solution was dialyzed exhaustively *versus* de-ionized water [Spectrapore 3 dialysis tubing, molecular-weight cutoff (m.w.c.o.) 3500], and lyophilized (yield, 55 mg; 38%).

(*c*) *Mannan (M_i and M_s) by Smith degradation of the xylomannan (XM)*[22]. XM (77 mg) was disolved in 77 mL of 0.04M $NaIO_4$ and kept for 96 h at 4° in the dark. Ethylene glycol (0.154 g) was added, and after 1 h $NaBH_4$ (0.288 g); the mixture was kept in a refrigerator for 24 h and the pH then adjusted to 5 with acetic acid. The soluble polyalcohol was recovered by lyophilization after exhaustive dialysis (yield, 55 mg; 71%). The polyalcohol was disolved in 0.1M HCl (2.5 mL) and

the solution kept overnight at 37°. The fine, white precipitate that formed was removed by centrifugation for 5 min at 1000*g*, washed successively with cold water (2×2 mL), 95% ethanol (2×2 mL), 100% ethanol (2 mL), and ether, and dried *in vacuo* (yield, 10.6 mg of M_i; 20% based on 77 mg of XM). The supernatant liquor and washings were combined, exhaustively dialyzed (Spectrapore 6, m.w.c.o. 1000) *versus* de-ionized water, and lyophilized (yield, 19.8 mg of M_s; 26% based on 77 mg of XM.

(*d*) *Polyalcohol (PM).* The procedure used to generate the polyalcohol derivative of GXM was similar to that used to prepare M in (c). However, in this case, the $NaBH_4$ reduction was conducted under pH control (see *h*), in order to retain the *O*-acetyl substituent, and the acid hydrolysis was eliminated entirely.

(*e*) O-*Deacetylated polysaccharides (DPM, DGXM, DGXMS, DRGXM, and DRGSMX).* Polysaccharide (PM, or other precursor polysaccharide) was dissolved in water (2 mg/mL) and the pH adjusted to 11 with concentrated NH_4OH. After 1 h at room temperature, the *O*-deacetylated polysaccharide was recovered by lyophilization.

(*f*) *Sonicated GXM (GXMS).* GXM (200 mg in 75 mL of de-ionized water) was sonicated for 15 min at 10° at a power setting of 8 and a 40% pulse (Cell Disruptor, Heat Systems Ultrasonics, Inc., Model W225R). The rate of heat transfer from the sample vessel to the surrounding cooling medium was not sufficient to maintain the initial temperature of 10° of the polysaccharide solution, but the temperature was not permitted to rise above 20° during the experiment.

(*g*) *Partial acid hydrolyzate of GXMS (PAHGXMS).* Following purification by gel filtration, GXMS was dissolved in 0.5M trifluoroacetic acid (100 mg in 10 mL) and heated for 30 min at 100°. The pH of the hydrolyzate was adjusted to 6, and the sample was recovered by lyophilization after dialysis (Spectrapore 6, m.w.c.o. 1000) *versus* de-ionized water (yield 75 mg, 75%). Any remaining *O*-acetyl groups were removed as in (*e*), and the lyophilized product was used without additional purification.

(*h*) *Reduced polysaccharides (RGXM and RGXMS)*[23]. The percursor polysaccharide (*e.g.*, GXMS) (100 mg) was dissolved in water (20 mL), and the pH adjusted to 4.7. 3-(3-Dimethylaminopropyl)-1-ethylcarbodiimide·HCl (77 mg) was slowly added during 1 h with stirring, while the pH was maintained between 4.7 and 5.0 by adding 0.05M HCl as needed. After additional stirring for 1 h, $NaBH_4$ (1.4 g) was added in small portions, keeping the pH between 7 and 8 by the dropwise addition of 4M HCl. In some instances, a few drops of octanol were needed in order to inhibit foaming. The reaction was permitted to proceed for 1 h with continued adjustment in pH as needed. The pH was adjusted to 6.5, and the reduced polysaccharide recovered by lyophilization after exhaustive dialysis *versus* de-ionized water (yield, 81 mg, 81%).

Gel filtration. — Xylomannan (144 mg) was dissolved in 0.05M 2-amino-2-(hydroxymethyl)-1,3-propanediol–0.1M NaCl (10 mL) buffer, pH 7.6, and the solution applied to a column (90 × 2.5 cm) of Sephacryl S-200 (Pharmacia) equili-

brated with the same buffer. The flow was 27 mL/h, the eluate was continuously monitored at 206 nm, and individual fractions were analyzed with phenol–sulfuric acid[24]. The column was calibrated with standard proteins with a molecular-weight range of 13,700 to 67,000 (Pharmacia, Gel Filtration Calibration Kit). The appropriate carbohydrate-containing fractions were combined, dialyzed *versus* de-ionized water, and lyophilized.

Other polysaccharides (*e.g.*, GXMS or its derivatives) were chromatographed as just described, except that Sepharose CL-6B (Pharmacia) was used instead of Sephacryl S-200. Standard proteins with a range of molecular weight of 158,000 to 669,000 (Pharmacia, Gel Filtration Calibration Kit) were used to calibrate the Sepharose CL-6B column.

Analytical methods. - Neutral carbohydrate was detected by the phenol–sulfuric acid method[24]. Glucuronic acid was determined by the *m*-hydroxydiphenyl reaction[25]. The constituent monosaccharides were identified and quantitated by methods previously described[10,26]. Polysaccharide was hydrolyzed with 2M trifluoroacetic acid; timed aliquots were removed, the acid was removed by extraction with moist ether (5 × 3 mL), and each monosaccharide concentration was extrapolated to zero time.

RESULTS

Polysaccharides. — Scheme 1 summarizes the origins of the various polysaccharides examined in this study and the definitions of their acronyms.

(*a*) *Glucuronoxylomannan.* — An *O*-acetylglucuronoxylomannan (GXM) was isolated from the extracellular polysaccharides and other components of the medium in a growth of *C. neoformans* (see Scheme 1, procedure a) as described previously[18]. Chemical and g.l.c. analyses revealed GXM to contain mannose, xylose, glucuronic acid, and *O*-acetyl groups in the molar ratios of ~10:4:3:6. No other chemical constituents were observed.

(*b*) *Xylomannan.* — A xylomannan (XM) was obtained by treatment of GXM with Li in ethylenediamine (Scheme 1, procedure b)[20,21]. The recovery of XM lay between 40 and 50%, based on GXM as starting material. The XM isolated was confirmed to be 90% depleted in GlcA when compared to native GXM by both colorimetric analysis and ^{13}C-n.m.r. spectroscopy. The molar ratio of mannose to xylose for XM was found by g.l.c. to be ~5:2. Elution of XM from a column of Sephacryl S-200 occurred in a single symmetrical peak. The peak width at half height was slightly greater than that observed for chymotrypsinogen; this suggests low polydispersity. The elution volume indicated that XM had an apparent molecular weight of 35,000.

(*c*) *Mannan.* — Smith degradation of XM (Scheme 1, procedure c) yielded a polysaccharide (M) which was composed only of mannose, as determined by g.l.c. Separation of M into two fractions of different water-solubility occurred during the mild acid-catalyzed hydrolysis. Both fractions were soluble in Me_2SO-d_6, which

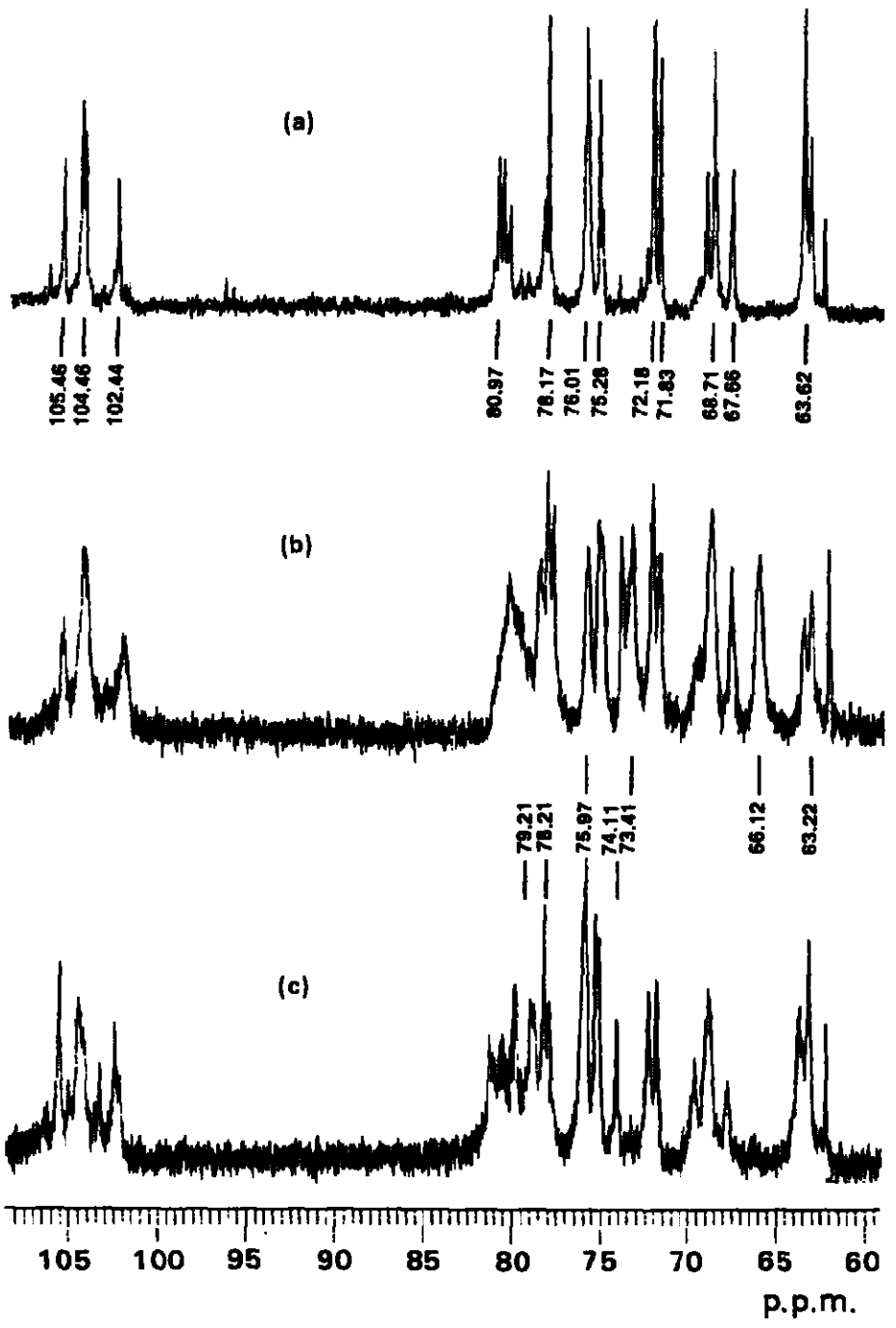

Fig. 1. Proton-decoupled ^{13}C-n.m.r. spectra of polysaccharides derived from GXM of *C. neoformans* serotype A-variant. Key: (a) Xylomannan, XM; (b) sonicated GXM, GXMS; (c) *O*-deacetylated GXMS, DGXMS.

facilitated the determination of their essentially identical ^{13}C-n.m.r. spectra.

(*d*) *Polyalcohol.* – Native GXM was subjected to oxidation with $NaIO_4$, followed by reduction with $NaBH_4$ at neutral pH (Scheme 1, procedure d), to give a polysaccharide (PM) that was water-soluble and contained *O*-acetyl and polyalcohol substituents, as evidenced by the ^{13}C-n.m.r. spectrum (see Fig. 3a).

(*e*) O-*Deacetylation.* — The *O*-acetyl groups were removed from PM, GXMS, and RGXMS (see *f*) by treatment with NH_4OH (Scheme 1, procedure e). This resulted in an *O*-deacetylated, water-soluble polysaccharide (DPM) from PM. Corresponding *O*-deacetylated polysaccharides DGXMS and DRGXMS were respectively formed from GXMS and RGXMS. Although *O*-acetyl groups were essentially completely removed, ^{13}C-n.m.r. spectroscopy indicated that the other structural residues were retained as side chains (see Figs. 1c, 2c, and 3b). For example, as indicated by

g.l.c. analysis, DRGXMS contained only Man, Xyl, and Glc in the expected ratios of ~5:2:1.

(*f*) *Sonication.* — A dilute aqueous solution of native GXM was subjected to ultrasonic irradiation to produce an approximately tenfold diminution in solution viscosity (GXMS; Scheme 1, procedure f).

(*g*) *Partial acid hydrolysis.* — Partial acid hydrolysis of GXMS produced no obvious physical changes (PAHGXMS; Scheme 1, procedure g).

(*h*) *Reduction of GXMS.* The reduction of the carboxylic acid groups of Glc*p*A to hydroxymethyl groups was achieved as shown in Scheme 1, procedure h. A single treatment was not sufficient to convert all of the glucuronic acid into glucose; the reaction was repeated three times to acheive complete reduction. Although the reduction was conducted under pH control, partial loss of *O*-acetyl substituents

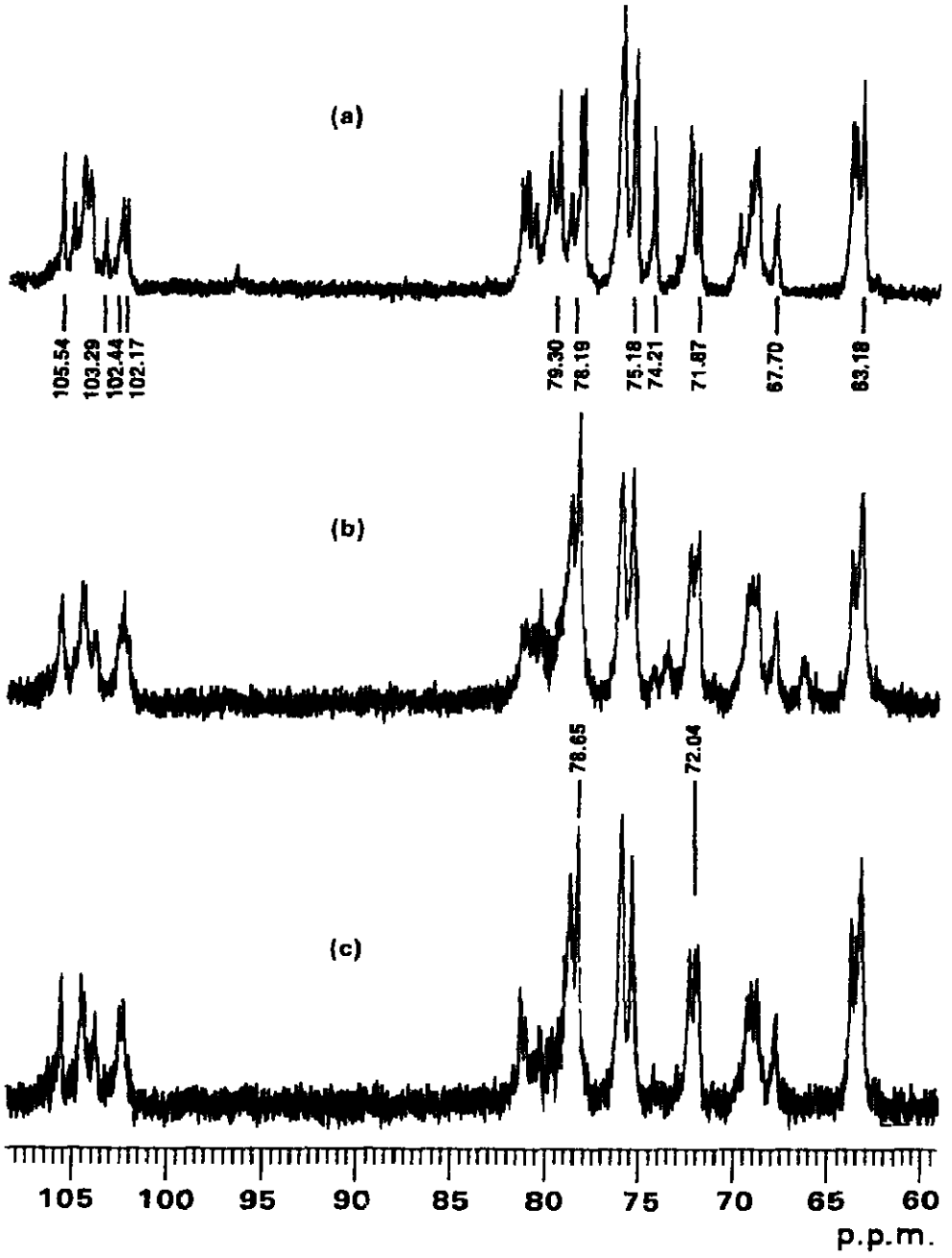

Fig. 2. Proton-decoupled ^{13}C-n.m.r. spectra of polysaccharides derived from GXM of *C. neoformans* serotype A-variant. Key: (a) Partial acid hydrolyzate of GXMS, PAHGXMS; (b) reduced GXMS, RGXMS; (c) *O*-deacetylated RGXMS, DRGXMS.

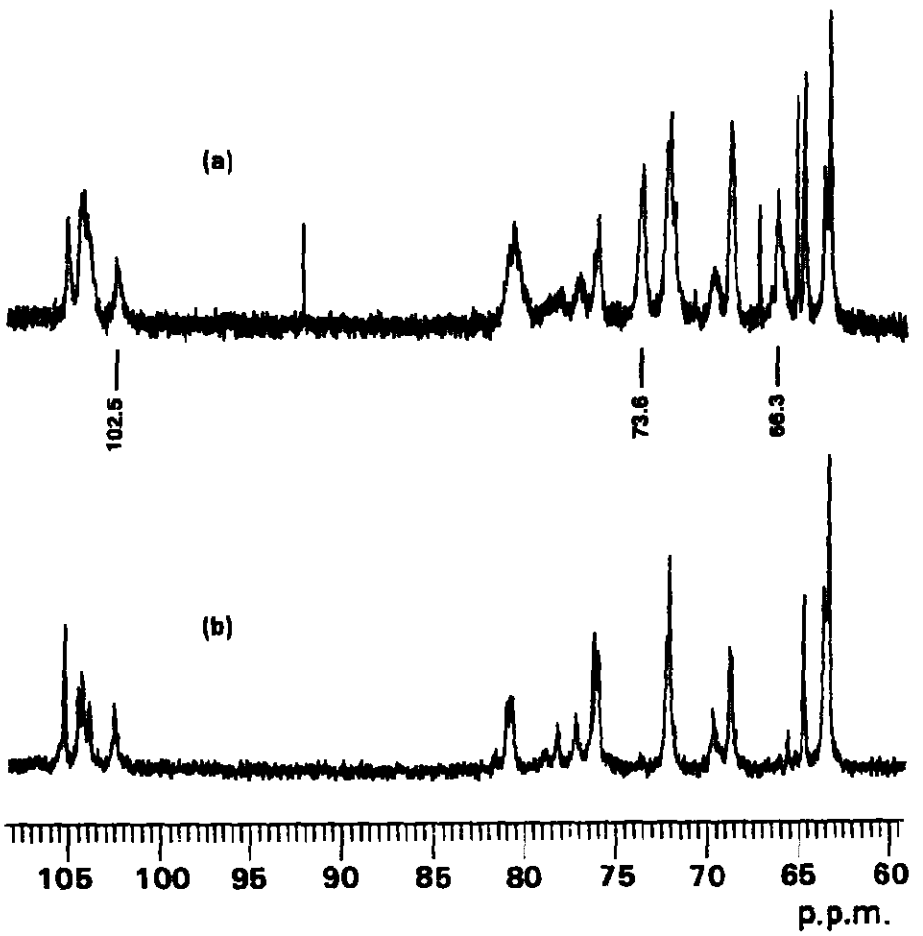

Fig. 3. Proton-decoupled, ^{13}C-n.m.r. spectra of polysaccharides derived from GXM of *C. neoformans* serotype A-variant. Key: (a) Polyalcoholmannan, PM; (b) *O*-deacetylated PM, DPM.

was observed by ^{13}C-n.m.r. spectroscopy.

^{13}C-N.m.r. spectra — Figs. 1–3 show the ^{13}C-n.m.r. spectra of some of the polysaccharides in Scheme 1. Tables I through III give the chemical shifts and selected C–H coupling constants for the polysaccharides, and for related reference saccharides.

Table I contains the ^{13}C-n.m.r. data observed for M_i and M_s in Me_2SO-d_6, and XM in D_2O (lines 3, 4, and 9, respectively). Similar comparative data observed for methyl α-D-mannopyranoside (Me α-Man*p*) in both D_2O and Me_2SO-d_6 and for methyl β-D-xylopyranoside (Me β-Xyl*p*) in D_2O are also included (lines 1, 2, and 10, respectively), as are literature and calculated values for two previously reported mannopyranans (lines 5–8).

Mannan M_s was not sufficiently soluble in D_2O for an efficient determination of its ^{13}C-n.m.r. spectrum. Consequently, the spectra of both M_i and M_s were determined in Me_2SO-d_6 and the chemical-shift values were recorded relative to the solvent resonance at 39.60 p.p.m. (Table I, lines 3 and 4, respectively). Both spectra revealed six well resolved signals of nearly equal intensities, with no evidence of additional minor signals. In Table I, lines 5 and 7 give data from the literature for comparable species. The values shown for MH in line 7 were derived from those reported by Hara *et al.*[27] by addition of 1.5 p.p.m. to the literature values in order to adjust them to the DSS reference.

The ^{13}C-n.m.r. data for XM (see Table I, line 9, and Fig. 1a) were determined

TABLE I

^{13}C-N.M.R. DATA FOR THE MANNANS M_s AND M_i, FOR THE XYLOMANNAN XM, AND FOR STRUCTURALLY RELATED SACCHARIDES

Line	*Saccharide*[a]	*Solvent*	*Temp.*	*Chemical shifts and* [Δδ] *in p.p.m. and* ($^1J_{CH}$) *in Hz*						
			(degrees)	*C-1*	*C-2*	*C-3*	*C-4*	*C-5*	*C-6*	CH_3
1a	Me-α-Man*p*[b]	D_2O	70	103.24	72.36	73.09	69.28	74.92	63.41	57.10
b				(170)	(149)	(144)	(151)	(142)	(143)	(144)
2a	Me-α-Man*p*[c]	Me_2SO-d_6	70	100.76	70.02	70.94	67.16	73.45	61.31	53.81
b				(167)	(145)	(142)	(145)	(138)	(140)	(142)
3a	M_i Man*p*-a[c]	Me_2SO-d_6	70	101.49	69.45	78.51	66.01	73.56	61.16	
b[d]				[0.73]	[−0.57]	[7.57]	[−1.15]	[0.11]	[−0.15]	
c				(171)	(147)	(140)	(149)	(143)	(140)	
4a	M_s Man*p*-a[c]	Me_2SO-d_6	70	101.44	69.41	78.46	65.98	73.51	61.10	
b[d]				[0.68]	[−0.61]	[7.52]	[−1.18]	[0.05]	[−0.21]	
c				(167)	(147)	(141)	(145)	(145)	(141)	
5	MK Man*p*-a[e]	Me_2SO-d_6	70	101.5	69.4	78.4	66.1	73.5	61.1	
6a	M Man*p*-a(Calc.)[f]	Me_eSO-d_6	70	100.68	69.60	78.39	66.46	73.50	—	
b	M_i Man*p*-a[g]	Me_2SO-d_6	70	[0.81]	[−0.15]	[0.12]	[−0.45]	[0.05]	—	
c	M_s Man*p*-a[g]	Me_2SO-d_6	70	[0.76]	[−0.19]	[0.07]	[−0.48]	[0.01]	—	
7a	MH Man*p*-d[h]	D_2O	68	104.3	72.1	80.5	68.6	75.9	63.6	
b	MH Man*p*-e	D_2O	68	104.3	72.1	80.5	68.6	73.5	66.1	
8a	MH Man*p*-a(Calc.)[i]	D_2O	30	104.4	72.1	80.3	68.6	75.7	63.4	
b	MH Man*p*-d[g]	D_2O	—	[−0.1]	[0.0]	[0.2]	[0.0]	[0.2]	[0.2]	
9a	XM Man*p*-a[j]	D_2O	70	104.32	72.18	80.69	68.71	76.01	63.62	
b				(174)	(150)	—	(150)	(149)	(144)	
c	XM Man*p*-b[j]	D_2O	70	104.46	—	80.97	68.57	—	—	
d				(170)	—	(144)				
e	XM Man*p*-c[j]	D_2O	70	102.44	80.32	80.97	69.13	76.15	63.24	
f[c]				[−2.02]	[8.14]	[0.28]	[0.56]	[0.14]	[−0.38]	
g				(171)			(146)		(144)	
h	XM Man*p*-c[j,k]	D_2O	70			78.39	68.57		63.62	
i	XM Xyl*p*[j]	D_2O	70	105.46	75.28	78.17	71.83	67.66		

TABLE I *(continued)*

j[f]				[−0.89]	[−0.01]	[−0.01]	[0.17]	[0.18]	
k				(160)	(147)	(147)	(148)	(139)	
10a	Me-β-Xyl*p*[b]	D_2O	70	106.35	75.29	78.18	71.66	67.48	59.31
b				(161)	(146)	(144)	(143)	(144)	

[a]The suffix letters in the saccharide abbreviations (*e.g.*, a in M_i Man*p*-a) refer to polysaccharide residues and have the following meanings: a, b, and d, are unsubstituted; c, is 2-*O*-β-D-xylosylated (see text); e, is 6-*O*-acetylated. [b]Measured relative to internal sodium 4,4-dimethyl-4-silapentane-1-sulfonate (DSS) at 0.00. [c]Measured relative to solvent, Me_2SO-d_6, at 39.60. [d]Chemical-shift change [(δMan*p*) − (δMe α-Man*p*)]. [e]MK, synthetic (1→3)-α-D-Man*p* with values measured relative to solvent Me_2SO-d_6 as noted in ref. 31. [f]Calculated by the method described in ref. 30, or an adaptation (see text). [g]Differentials between the observed and calculated chemical shifts. [h]MH (see text) values from ref. 27, measured relative to internal, 1,4-dioxane taken as 67.4, were adjusted to the DSS scale by the addition of 1.5. [i]Calc. by the method described in ref. 30 and adjusted to DSS reference by addition of 1.04. [j]Measured relative to external DSS taken as 0.00. [k]Alternative values. [l]Chemical-shift change [(δXyl*p*) − (δMe β-Xyl*p*)].

TABLE II

^{13}C-N.M.R. DATA FOR SIDE-CHAIN GROUPS OF GXM DERIVATIVES AND FOR REFERENCE SACCHARIDES

	Saccharide and residue		*Chemical shifts in p.p.m.*[a]						
			C-1	*C-2*	*C-3*	*C-4*	*C-5*	*C=O*	*CH$_3$*
1a	Me β-Xyl*p*[b]	β-Xyl*p*	106.35	75.29	78.18	71.66	67.48		59.31
b	XM		105.46	75.28	78.17	71.83	67.66		
c	PAHGXMS		105.54	75.30	78.19	71.87	67.70		
d	DGXMS		105.55	75.32	78.21	71.87	67.72		
e	DRGXMS		105.56	75.37	78.24	71.91	67.73		
f	GXMS		105.57	75.32	78.24	71.87	67.72		
g	RGXMS		105.58	75.37	78.24	71.88	67.72		
2a	Me β-Glc*p*A[c]	β-Glc*p*A	105.8	75.3	78.0	73.8	77.1	179.1	60.0
b	*p*-NO$_2$Ph β-Glc*p*A		102.31	75.34	78.02	74.26	78.74	177.45	
c	XM		104.83	75.13	77.97	74.16	79.29	177.45	
d	PAHGXMS		105.01	75.18	78.00	74.21	79.30	177.54	
e	DGXMS		104.98	75.14	77.94	74.11	79.21	176.80	
f	DRGXMS		104.96	—	77.94	74.22	—	—	
g	GXMS		104.96	75.32[d]	77.87	74.05	79.28	—	
h	RGXMS		104.92	—	—	74.22	—	177.55	
3a	Me β-Glc*p*[c]	β-Glc*p*[e]	105.5	75.6	78.3	72.1	78.3		59.6
b	RGXMS		104.51[f]	75.37[d]	78.64	72.08	78.64		
c	DRGXMS		104.54[f]	75.37[d]	78.65	72.04	78.65		
4a	GXMS	*O*-Acetyl						176.12	23.00
b	RGXMS							176.28	23.10
c	PM							176.11	22.89

[a]Relative to external sodium 4,4-dimethyl-4-silapentane-1-sulfonate (DSS) unless otherwise indicated. In some polysaccharides, the levels of some side-chain groups were very small, as were the corresponding signals. [b]Relative to internal DSS. [c]Values from reference 41 were adjusted to the DSS reference by addition of 1.5. [d]Composite signal with a β-Xyl*p* resonance. [e]C-6 chemical shifts for: 3a, 63.3; 3b, 63.33; 3c, 63.25. [f]Composite signal with an α-Man*p* resonance.

for solutions in D_2O, and the chemical shifts were measured relative to external DSS. There was no evidence of the presence of methyl signals in the upfield 20-p.p.m. region of the spectrum of XM that might be attributed to *O*-acetyl groups (not shown). In addition to the chemical-shift values given in Table I, line 9, other minor signals, having intensities $<13\%$ of that of the most intense signal (at 63.62 p.p.m.), were observed, but are not presented in Table I; some of them are shown in Fig. 1a. Three minor signals were observed, at 177.45 (not shown), 96.39, and 95.89 p.p.m., with respective intensities of ~ 7, 11, and 8% of that of the signal at 63.62 p.p.m. Tables II and III show the relationship between the resonances observed for XM and the other GXM derivatives. Data for reference compounds, side-chain groups, and mannosyl residues of the various compounds identified in Scheme 1 are given in the Tables.

TABLE III

^{13}C-N.M.R. DATA FOR α-MANNOPYRANOSYL MOIETIES OF GXM DERIVATIVES

	Saccharide	*Chemical shift in p.p.m.[a] of carbon atoms in designated Man units*							
1		*C-1 of units that are*							
		Unsubstituted				*2-O-Glycosylated with*			
						β-Xyl	*β-Glc*	*β-GlcA*	
a	XM	104.46	104.32			102.43			
b	PAHGXMS	104.49	104.40	104.12	103.29	102.44		102.17	
c	DGXMS	104.45		103.55	103.27	102.41		102.17	
d	DRGXMS		104.35	103.80	103.27[b]	102.51	102.31		
e	GXMS		104.36			102.56		102.16	
f	RGXMS	104.51	104.37	103.86		102.56	102.31		
g	PM[c]	104.43	104.31	104.17		102.52			
h	DPM[c]	104.51	104.32	103.93		102.52			
2		*C-2 of unsubstituted units*							
a	XM	73.00[b]		72.59[b]			72.18		
b	PAHGXMS	72.97[b]				72.34			
c	DGXMS			72.53[b]		72.36			
d	DRGXMS	72.98[b]				72.36			
e	GXMS	72.90[b]	72.81[b]				72.25		
f	RGXMS				72.40	72.36			
g	PM			72.59[b]			72.21	72.06	
h	DPM						72.19	72.08	
3		*C-3 and C-2 of 2-O-glycosylated units[d]*							
a	XM	81.21	80.97	80.69	80.47	80.31	79.72		78.39
b	PAHGXMS	81.25	80.97		80.59		79.77		78.69
c	DGXMS	81.27			80.57		79.79	78.95	
d	DRGXMS	81.24	81.01			80.34	79.64	78.95	
e	GXMS					80.37		78.71–78.60	
f	RGXMS	81.27	81.0		80.46	80.30			
4		*C-4 of units that are*							
		2-O-Glycosylated					*Unsubstituted*		
a	XM			69.51[b]		69.13		68.71	68.57
b	PAHGXMS		69.70			69.19	68.95	68.82	68.69
c	DGXMS		69.60				68.90	68.71	
d	DRGXMS		69.72[b]		69.26	69.12		68.79	68.46
e	GXMS	69.96[b]	69.70[b]	69.49[b]		69.05	68.90	68.81	
f	RGXMS		69.81[b]	69.48	69.28	69.07		68.78	68.40[b]
g	PM3			69.63				68.73	
h	DPM			69.66				68.73	

TABLE III *continued*

5		*C-5 of units that are*							
		Unsubstituted						*6-O-Acetylated*	
a	XM	76.15	76.01	75.89					
b	PAHGXMS		75.99	75.87					
c	DGXMS			75.88					
d	DRGXMS			75.92					
e	GXMS		75.97					73.41	
f	RGXMS		75.96					73.46	
g	PM	76.27	76.02					73.58	
h	DPM	76.22	76.02						
6		*C-6 of units that are*							
		6-O-Acetylated		*Unsubstituted*			*2-O-Substituted*		*Others*
a	XM			63.62			63.24		62.44
b	PAHGXMS			63.17	63.56				63.18
c	DGXMS			63.72			63.20		62.19
d	DRGXMS			63.75			63.25		
e	GXMS		66.12		63.64		63.22		62.22,62.09
f	RGXMS		66.18	63.73			63.22		
g	PM[e]	66.32–66.21			63.63		63.32		
g	DPM[e]				63.62	63.46	63.35		

[a]Relative to external sodium 4,4-dimethyl-4-silapentane-1-sulfonate taken as 0.00. [b]Signals with low relative intensity, for minor components. [c]C-1 resonance of Xyl group, 105.2. [d]The resonance not listed at ~79.3 for XM, PAHGXMS, and DGXM is due to C-5 of GlcA and that at ~78.6 for DRGXMS and RGXMS is due to C-3 and/or C-5 of Glc (see Table II, lines 2c–e and 3b,c. [e]Other, unassigned resonances for: 6g, 64.73, 65.15, 67.22; 6h, 63.46, 64.73.

DISCUSSION

Correlations of ^{13}C-n.m.r. chemical shifts of mannosyl residues with structural features in mannans were studied by Gorin[28,29], with emphasis on the anomeric region of the spectrum (90–110 p.p.m.). Allerhand and Berman[30] extended these studies to the entire spectrum. The results are useful for calculating chemical shifts of model structures of complex carbohydrates. In this study, the base ^{13}C chemical-shift values of Allerhand and Berman[30] were adjusted to the DSS reference by the addition of 1.04 p.p.m. Mannosylation shifts[30] for changes in ^{13}C chemical-shifts upon α-D-mannosylation of α-D-mannopyranosyl residues were employed without change.

Structure of the Mannan (M). — The spectra for M_i and M_s were essentially identical; thus, they are not significantly different structures, but rather M_i was the residue from a saturated aqueous solution of M_s. The appearance of only six discrete signals showed that M is a homopolymer having all of its mannosyl residues identically linked (see Table I, lines 3a and 4a). Comparison of the coupling con-

stants of the signals in the anomeric-carbon region of the spectra of the two mannan fractions with that of Me α-Man*p* unequivocally established the configuration of the anomeric centers of M to be α (see Table I, lines 1–4; J_{CH} values for C-1). The chemical shifts assigned here for the fractions of M are virtually identical to those reported by Kong and Schuerch[31] for a synthetic, stereoregular (1→3)-α-D-mannopyranan (see Table I, line 5). The also agree with calculated values (see Table I, line 6) as described later.

The method of Allerhand and Berman[30] was adapted for use with Me_2SO-d_6 as the solvent; carbon chemical shifts observed for Me α-Man*p* in Me_2SO-d_6 (see Table I, line 2) were used as base values, rather than those recommended in Table VI of ref. 30 for D_2O solutions. The 3-*O*-α-mannosylation chemical shift changes from Table V of ref. 30 were used. The calculated chemical-shifts for a structure constituted only of α-(1→3)-Man*p* linkages are given in Table I, line 6. The differences between the observed and calculated values are also given (see Table I, lines 6b and c). Other than values for the anomeric center, which in mannosyl residues is known to be sensitive to substituent effects, the largest differential is for C-4. The chemical shift for this carbon atom may exhibit solvent effects due to differences in rotamer population of the CH_2OH group in Me_2SO-d_6 and D_2O, or in H-bonding properties of the nonsubstituted OH-4 group that may parallel the differences in solubility observed for M in water *versus* Me_2SO-d_6.

The spectrum of the mannan in aqueous solution is not available due to low solubility in water. Hara *et al.*[27] isolated a water-soluble 6-*O*-acetylated (1→3)-α-D-mannopyranan (MH) from the fruit bodies of *Dictyophora indusiata* Fisch. The structure found for MH is the same as that of the synthetic homopolymer[31] mentioned, except that, in MH, *O*-acetyl groups are linked to *O*-6 of the backbone and occur on about one of every two Man*p* residues. The chemical shifts for nonacetylated and acetylated Man*p* residues of MH are given in Table I, line 7, as MH Man*p*-d and Man*p*-e, respectively. Also given, as MH Man*p*-a (Calc.) (Table I, line 8a), are values calculated for D_2O solutions by the method of Allerhand and Berman[30]. The differentials between the calculated and observed values (Table I, line 8b) indicate better applicability of the calculations for aqueous than for Me_2SO-d_6 solutions. The *O*-deacetylation of MH gave a water-insoluble mannan[27]. The related synthetic mannopyranan[31] was also water-insoluble, as was M. These solubility factors resulted in the use of different solvents in the spectral determinations of these mannans and complicate comparison of their chemical shifts. Nevertheless, there is good agreement among the n.m.r. data and good agreement between the experimental data and the calculated values (see Table I, lines 3–8). This suggests that all three polysaccharides are (1→3)-α-D-mannopyranans, except for the frequent presence of 6-*O*-acetyl substituents in MH. This must also represent the backbone mannan structure of GXM as well as of XM and other GXM derivatives reported herein and probably accounts for the primary, if not exclusive, role of Man in GXM. Although present data do not unequivocally exclude other minor structural roles of Man, the data supporting the structure of XM also justify this conclu-

sion (see later).

Conformational constraints in the mannopyranan. — The (1→3)-α-D-mannopyranan is considerably less soluble in water than are either the partially 6-*O*-acetylated analog[27] or the partially 2-*O*-xylosylated analog (see XM in Scheme 1) discussed later; therefore, questions arise regarding whether conformational properties might contribute to these differences. Ealing CPK models (The Ealing Corporation) for the mannopyran constructed with exclusive $^4C_1$ (D) conformations for all of the Man*p* residues suggest that there may be two or more minimal-energy conformations for the polysaccharide. These conformations differ through simple rotations around the connecting glycosidic bonds, through variations in the dihedral angles ϕ at H 1′-C-1′-O-3-C-3 and ψ at C-1′-O-3-C-3-H-3 (ref. 32), as identified in **1**. The insolubility of the mannopyranan necessitated an indirect approach to the experimental study of its conformations by Ogawa *et al.*[33]. These workers reported X-ray diffraction results for a physically modified (1→3)-α-D-mannan dihydrate film from a partially *O*-acetylated mannan maintained as a film in the solid state during chemical modification. The geometry at the anomeric centers was found to be similar to that for the α-D-Man*p*(1→3)-α-D-Man*p* moiety in a trisaccharide measured by X-ray diffraction of crystalline material[34].

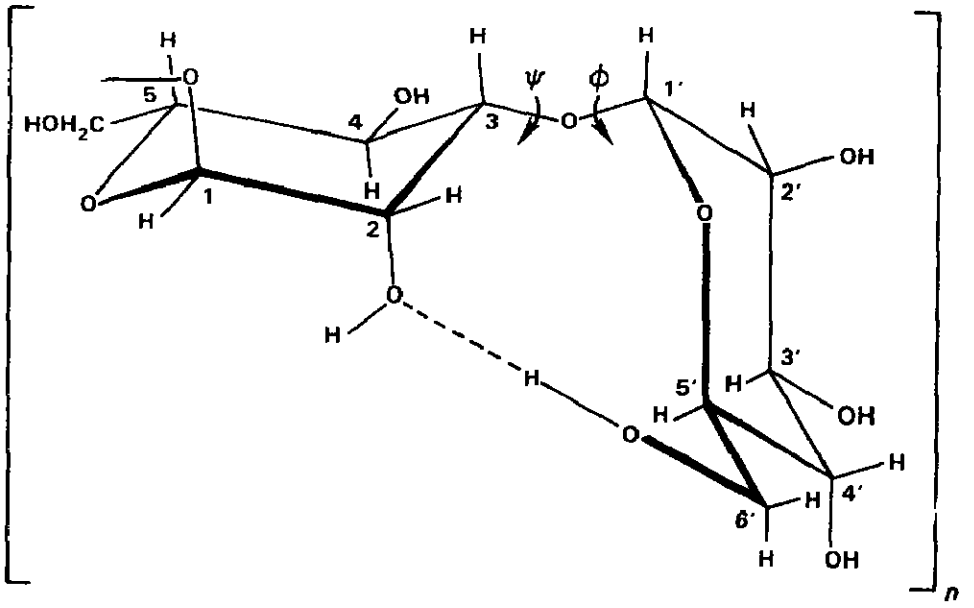

1

Because there are no definitive experimental conformational data on the mannopyranan, and as one of the anomeric orientations indicated by CPK models was not included in the potential energy map of (1→3)-α-mannobiose by Brisson and Carver[35], a new map has been calculated. The atomic coordinates of the mannobiosyl moiety from the X-ray crystal data for the trisaccharide mentioned[34] were used as a beginning approximation of the geometry of *O*-α-D-mannopyranosyl-(1→3)-α-D-mannopyranose. The molecular mechanics program MM2 (ref. 3b) was used without restriction of atomic positions to minimize the potential energy for the free structure of the biose at a variety of values for the dihedral angles ϕ and ψ. The starting values were chosen in pairs along a line having a slope of ~45° on the

anticipated contour map ($\phi = \psi + 50°$, where a dihedral angle of 0° represents an eclipsed, *cisoid* orientation for the first and fourth atoms of the dihedral angle of concern, and where a positive dihedral angle would require a clockwise rotation about the central bond to restore the dihedral angle to the *cis* orientation). At each minimum, a pair of rigid-rotor approximations (for ϕ and ψ, 360° rotations each) was made, and the potential energies were recorded at torsion-angle increments of 1° or 5°, with smaller increments employed near the geometry yielding the minimized potential-energy value. Construction of a preliminary contour map from these data revealed three unique areas of anomeric orientation with similar potential-energy minima. Each area was investigated in finer detail by varying the starting values of the angles further, and by examining alternative orientations of the peripheral C-*O*-H and C-5-C-6 moieties in search of the lowest potential-energy value. This permitted refinement of the contour map as shown in Fig. 4.

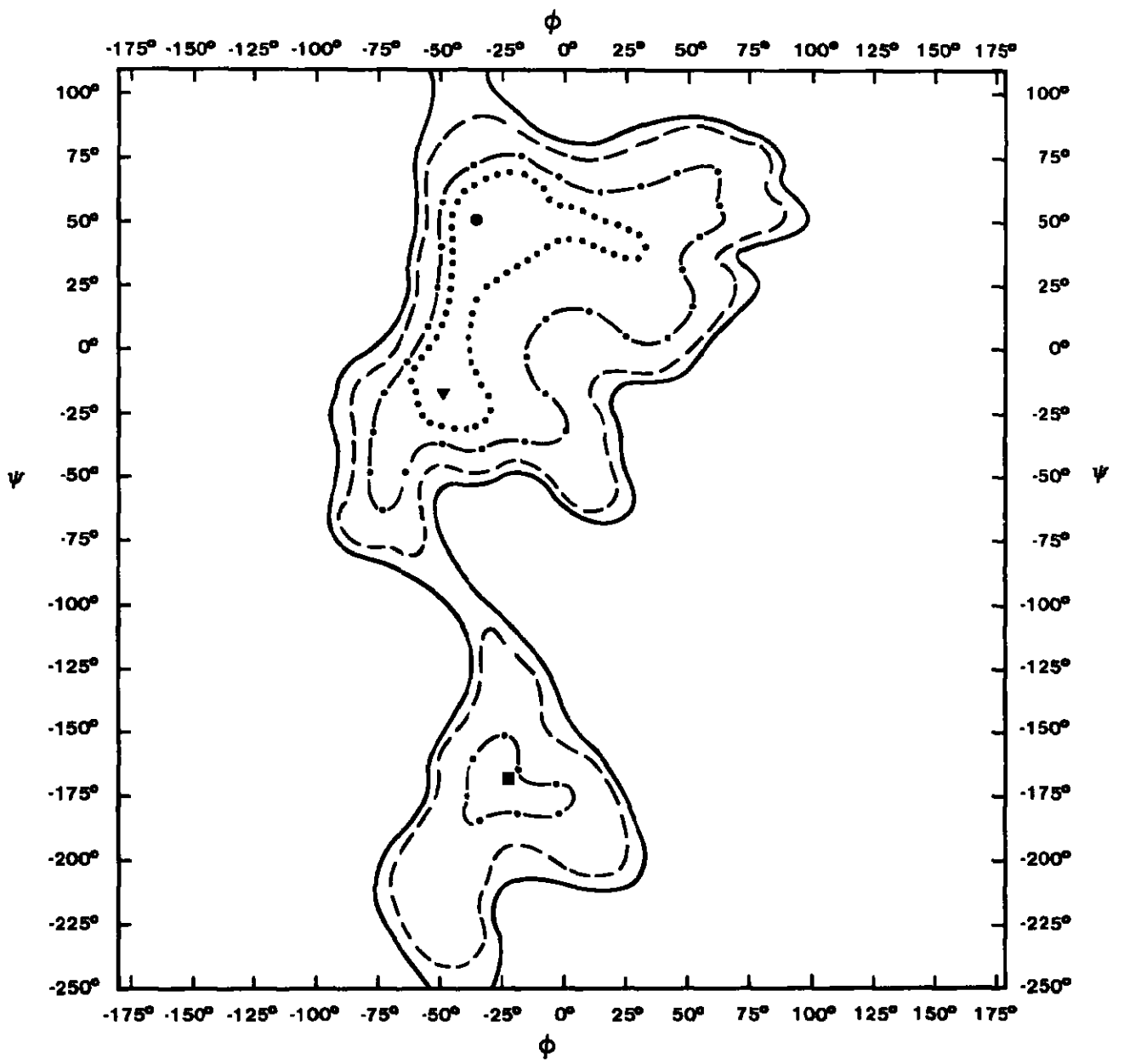

Fig. 4. Calculated potential-energy contour-surface for *O*-α-D-mannopyranosyl-(1→3)-α-D-mannopyranose, showing variations in the glycosidic orientation as determined by the dihedral angles (ϕ and ψ) and as evaluated by the molecular mechanics program MM2. The relative energy values of the minima and contour lines are: ●, I, 0.0 kJ.mol^{-1}; ▼, II, 11.5 kJ.mol^{-1}; ■, III, 22.2 kJ.mol^{-1}; ····, 14.6 kJ.mol^{-1}; -.-., 27.2 kJ.mol^{-1}; ----, 52.3 kJ.mol^{-1}; and ——, 69.0 kJ.mol^{-1}. Values of Φ and ψ outside the solid line contour were associated with orientations calculated to be of potential energies much higher than 69.0 kJ.mol^{-1}.

The estimated values of the relative potential energies for the three minima shown as I ($\phi = -36$, $\psi = 51°$), II ($\phi = -49°$, $\psi = -16°$), and III ($\phi = -22°$, $\psi = -168°$) in Fig. 4 are: 0, 12, and 22 kJ.mol^{-1}, respectively. Interconversion of the structure between minima I and II is not impeded by torsion barriers of significant magnitude. The relative potential-energy value of 14 kJ.mol^{-1} was computed for transition through the valley separating I from II on the contour map. A large area on the contour map near minima I and II is relatively unchanged in potential energy; various similar anomeric orientations are feasible near the geometries of I and II. Conversion of the structure from minimum I or II into III is impeded by a torsion barrier of greater significance. These barriers for I into III or II into III through the elevated energy valleys shown in Fig. 4 are ~57 kJ.mol^{-1}. Previous data[35] similar to that in Fig. 4 included two minima similar to I and II and their feasible interconversion, but with reversed potential energies, and no indication of the existence of minimum III.

Although in its present use MM2 was not refined for any special analysis of hydrogen-bonding effects, the detailed geometries calculated for the mannobiose in minima I and III both suggest that intramolecular hydrogen-bonding is feasible, namely, OH-6′---O-2 for minimum I and OH-6′---O-4, for minimum III. The calculated internuclear distances for minimum I were: O-6′---O-2, 32.0 nm; OH-6′---O-2, 23.9 nm. The analogous values for minimum III were: O-6′---O-4, 33.0 nm; OH-6′---O-4, 26.4 nm. Each of these orientations could be further stabilized beyond the MM2 calculation through hydrogen bonding.

Were the orientation of the mannobiose in each of the minima adopted in a repeating unit in the mannopyranan chain, with inter-residue H-bonding when indicated, three distinctly different minimal-energy conformations would result.

1. The mannopyranan conformation thus indicated by minimum II would be that of a twofold helical structure, probably much like that found in the X-ray study[33], but, according to the MM2 calculations, this conformation would be very flexible and perhaps be able to assume other conformations, including the new minimal-energy conformation related to minimum I.

2. The second mannopyranan conformation having the minimum I mannobiose as a repeating unit would be a left-handed, threefold helical structure with each OH-6′---O-2 H-bond intact. A CPK model of this conformation suggests that it is a rigid rod-like structure, and that parallel strands could be easily packed together (see Fig. 5, left). This model is especially attractive, because the presence of either 6-*O*-acetyl or 2-*O*-xylopyranosyl groups would disrupt the OH-6′---O-2 H-bonding, would lessen the ability for packing of parallel strands, and would produce increased solubility in water, as is observed for these derivatives.

3. The third mannopyranan conformation related to minimum III would be a right-handed helical structure, but with a much more gentle twist around the helical axis than in *2* and with all of the O-2 atoms located on the (shorter) inside edge of the molecular ribbon and oriented toward the helical axis (see Fig. 5, right). This conformation does not appear to be a realistic possibility for the mannopyranan,

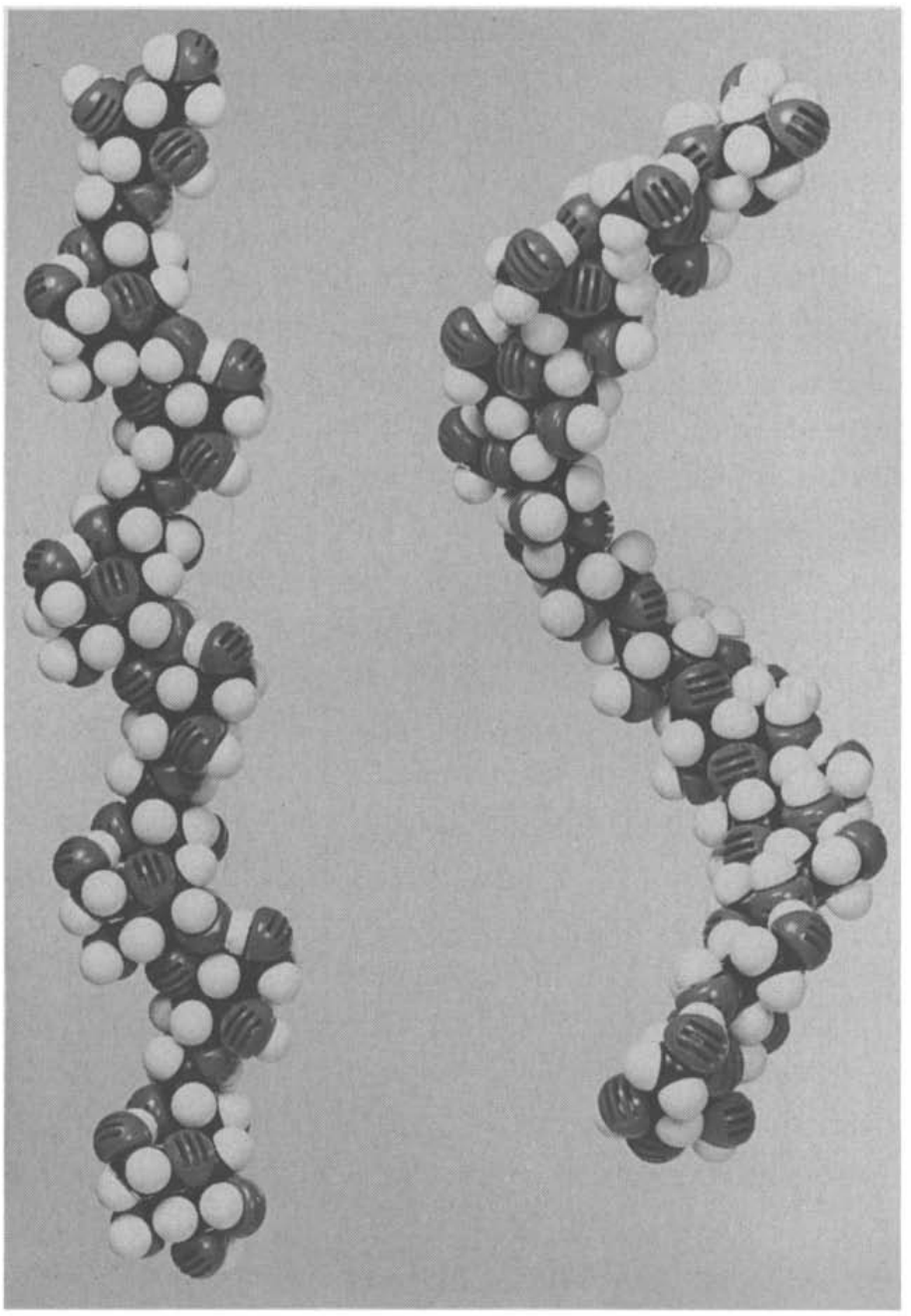

Fig. 5. CPK models of two theoretical minimal-energy conformations of (1→3)-α-D-mannopyranan, each with 12 Man*p* residues. The reducing termini are at the top of the photograph. Left, the conformation based upon the energy minimum I of Fig. 4, a rigid left-handed helical structure with a vertical threefold helical axis, showing two ridges of OH-6′---O-2 H-bonding along the outermost edges. A third identical ridge exists out of view on the back side of the model. Right, the conformation based upon the energy minimum III of Fig. 4, a flexible right-handed helical structure showing OH-6′---O-4 H-bonding in the foreground at the bottom of the structure and continuing upward along the outermost edge of the helical ribbon out of view on the back side of the middle section but reappearing in the foreground at the top of the model.

because of the higher relative potential-energy value associated with minimum III, and because of the barrier heights separating minima I or II from III. However, the presence of β-D-xylopyranosyl groups linked to O-2 atoms on the mannopyranan would appreciably alter the energetics of the polymer and might cause this conformation to be more feasible.

Structure of the xylomannan (XM). — Because XM was the precursor of M (see Scheme I, procedure c), it may be assumed that the primary structural role of the mannosyl residues is the same in the two polysaccharides. Additional Man*p* roles

in XM are excluded for more than a small percentage of the mannose. The ^{13}C-n.m.r. spectrum (see Fig. 1a) of XM exhibits a signal of low intensity at ~73.1 p.p.m., presumably due to C-3 of a minor proportion of nonreducing α-Man*p* residues (see Table I, line 1a) present in the structure of XM. The ratios of Man:Xyl in GXM and XM were found to be essentially constant. This indicated the loss of only GlcA substituents from the original structure, as expected from the chemical modification used (see Scheme 1, procedure b). These facts and the spectrum of XM (see Fig. 1a) are consistent with Structure 2, namely, a mannan backbone identical to the structure of M, with frequent, and probably regular, occurrence of β-Xyl*p* substituents attached to O-2 atoms of the backbone as discussed later.

The anomeric-carbon region of the spectrum of XM (see Fig. 1a) shows four intense resonances and one or more minor signals. The two intense signals at ~104.4 p.p.m. compare well with the C-1 signal of MH (see Table I, line 7) and result from C-1 resonances of Man*p* residues which are nonsubstituted by Xyl groups (see Structure 2, residues Ma and Mb). The anomeric signal at 105.46 p.p.m. is due to β-Xyl*p* substituents because of the following. The mannosylation of α-Man*p* residues discussed by Allerhand and Berman[30], and by Gorin[28,29], produced downfield shifts of the C-1 resonance of Man*p* residues that did not exceed 0.2 p.p.m. Thus, the resonance at 105.46 p.p.m. is not due to a Man*p* unit. Furthermore, the C-1 resonance of Me β-Xyl*p* is at 106.35 p.p.m. (see Table I, line 10). An aglycon larger than methyl would result in a smaller chemical shift for C-1 of Xyl*p*, as is observed at 105.46 p.p.m. Comparison of the C–H coupling constant (160 Hz) observed for this signal (see Table I, line 9k) with that (161 Hz) of methyl β-Xyl*p* (see Table I, line 10b) corroborates the β-anomeric configuration of the Xyl*p* groups of XM.

The XM signal at 102.44 p.p.m. (see Table I, line 9e) is due to C-1 of an α-Man*p* backbone residue (J_{CH} 171 Hz) substituted at O-2 with a β-Xyl*p* group. The chemical shift of this signal is 2 p.p.m. upfield from the signal of the nonsubstituted Man*p* residues. This upfield shift is appropriate for C-1 of α-Man*p* residues with 2-*O*-glycosyl substituents[29,30]. Therefore, the majority of the β-Xyl*p* substituents are attached to O-2 atoms of the mannan backbone in the structure of XM.

The minor anomeric signal, at 106.30 p.p.m., of XM (see Fig. 1a) also appeared in the spectrum of a second sample of XM prepared in an identical manner. This signal is due to β-Xyl*p* attached to O-4 atoms of the mannan backbone. Although evdence for such microstructure has not previously been offered for GXM derived from serotype A strains, present GC-MS data on permethylated XM indicate that ~9% of the Xyl*p* groups are attached to Man*p* O-4 atoms.

The nonanomeric region (60–82 p.p.m.) of the spectrum of XM (Fig. 1a) contains four signals with chemical-shift values within 0.2 p.p.m. of those for C-2 through C-5 of methyl β-xylopyranoside (Table I, lines 9i and 10a). Three of the signals have smaller linewidths than any others in the spectrum, as expected for Xyl*p* substituents with substantial motional freedom. The fourth broadened signal occurs at 67.66 p.p.m. These four signals are assigned to β-Xyl*p* groups attached to O-2

centers of the mannan backbone of XM.

There are five intense nonanomeric XM signals other than those assigned to Xyl*p* (Table I, line 9a). These agree with MH signals (Table I, line 7), and can be tentatively assigned to non-xylosylated α-Man*p*-a and α-Man*p*-b residues of the mannan backbone of XM (see structure **2** and Table I, lines 9a and 9c).

β-Xylosylation of a third of the O-2 centers of the mannan would be expected to produce some signals from carbon atoms of the xylosylated Man*p* residues. The signals would be of lower intensity than those of the β-Xyl*p* substituents due to the greater motional freedom of the latter. Furthermore, their approximate location can be anticipated from 2-*O*-substituent shift data for α-Man*p* residues[29,30]. Tentative assignments for these signals are given in Table I, line 9a, as are the observed substituent chemical-shifts (Table I, line 9f).

An alternative assignment for C-2 of the 2-*O*-xylosylated Man*p*-c is the signal at 78.39 p.p.m. with a xylosylation chemical-shift of only 6.2 p.p.m. However, this is probably not a Man*p* signal but that of a second Xyl*p* C-3 resonance produced by an unexplained proximity effect, because the ^{13}C-n.m.r. spectrum of the mannan from *Saccharomyces cerivisiae,* having a variety of (1→2)-, (1→3)-, and (1→6)-α-mannobiose linkages[37], exhibits no signals between 76 and 80 p.p.m. The assignments for C-2 and C-3 of Man*p*-c, while not unequivocal, are undoubtedly due to signals for the xylosylated Man*p* residues, and reversal of their assignments would not change the conclusion that the β-Xyl*p* substituents are attached to Man*p* O-2 atoms.

There are several minor signals observable in the XM spectrum in Fig. 1a. Most of these can be attributed to reducing and nonreducing α-Man*p* residues, to a small residual amount of β-Glc*p*A (Table II, line 2c) and the 4-*O*-β-Xyl*p* substituents, or to the α-Man*p* residues to which they are attached.

The structure of XM is represented generally by structures **2**, **3**, **4**, or **5**, where Ma, Mb, and Mc represent α-(1→3)-linked D-Man*p* residues of the backbone, and X represents 2-*O*-β-D-Xyl*p* substituents. These structures are consistent with the molar ratio (5:2) of Man:Xyl and the ^{13}C-n.m.r. data, and indicate that there are three unique environments for the Man*p* residues. Because there was no indication from the ^{13}C-n.m.r. data that the 2-*O*-β-Xyl*p* substituents occur regularly on adjacent Man*p* residues, structures **2**–**5** indicate that they occur on alternating Man*p* residues or are even farther removed from each other along the mannopyranan backbone. Two fundamental differences exist between the structures. One is whether XM is viewed as arising from the tetrad MaMbMc-X with missing Ma residues, as in structures **2** and **3**, or whether it is viewed as arising from the triad MbMc-X with missing X residues generating the MaMa unit from the MbMc unit, as shown in structures **4** and **5**. The second difference is whether the M residues occur in a regular, a block, or a random pattern. Current data do not permit detemination of whether the Ma residues occur alone, in pairs, or in aggregates of higher order. Thus, differentiation between these structures is not possible at present. The ^{13}C-n.m.r. data indicate that, when a Xyl*p* group occurs on the mannopyranan

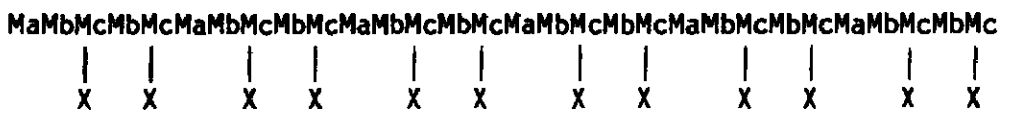

2

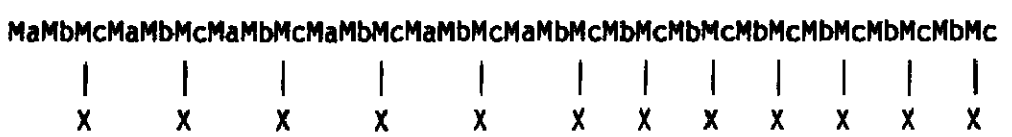

3

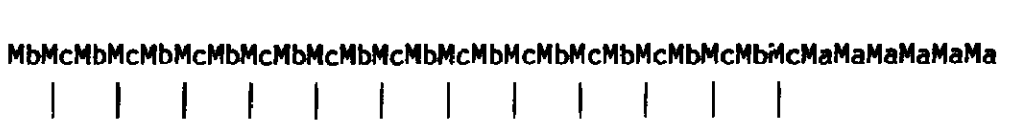

4

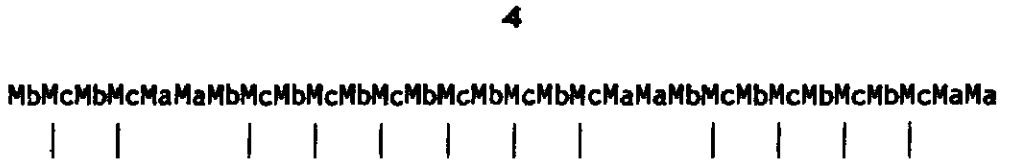

5

backbone, the chemical shifts of the Man*p* residue that is xylosylated (Man*p*-c) are shifted, and some of the chemical shifts of the adjacent, non-xylosylated Man*p* residues are also affected.

Structure of the sonicated native polysaccharide (GXMS). — High solution-viscosity made determination of a definitive ^{13}C-n.m.r. spectrum for GXM in D_2O at neutral pD impractical. Consequently, GXM was modified through reduction and *O*-deacetylation as shown in Scheme 1.

Sonication of GXM (Scheme 1, procedure f) lessened the apparent solution-viscosity, and improved the results. The ^{13}C-n.m.r. spectrum of GXMS (Fig. 1b) exhibits broad signals that are difficult to assign to specific carbon resonances, as they frequently represent overlapping, multiple absorptions. However, the C-1 resonances of β-Xyl*p* substituents and α-Man*p* residues can be observed to be almost unchanged from their positions in the spectrum of XM (Fig. 1a). Four signals are also observed at virtually identical positions, and have been assigned to C-2 through C-5 of β-Xyl*p* substituents in XM. The broadened spectral signals of GXMS are apparently due to the high viscosity of the solution. This seems to be due in part to the presence of the *O*-acetyl groups as their removal (to give DGXMS) further improved the spectrum (Fig. 1c). A greater improvement was obtained for PAHGXMS (Fig. 2a), through decreased viscosity that resulted from partial depolymerization of GXMS. The spectra of DGXMS (Fig. 1c) and PAHGXMS (Fig. 2a) are very similar, and exhibit more clearly resolved signals than does that of GXMS (Fig. 1b).

The five signals attributable to the β-Xyl*p* substituents are easily identified in both of the spectra (Figs. 1c and 2a), and in those of RGXMS and DRGXMS (Fig.

2b,c). The constancy of chemical shifts for these signals, shown in Table II, lines 1b–g, and their essentially constant relative intensities seen in the various spectra, suggest that the β-Xyl*p* groups bear no substituents.

Table II, lines 2c–h, contains tentative assignments for six signals from carbon atoms of β-Glc*p*A in the various spectra. In the spectra of XM, DRGXMS, and RGXMS, these signals were present only at low intensity and verified the incomplete removal of GlcA in XM or incomplete conversion into Glc in RGXMS and DRGXMS. Because β-Xyl*p* substituents are probably more labile to acid-catalyzed hydrolysis than are β-Glc*p*A substituents, the ratio of Glc*p* to Xyl*p* would be expected to be greater in PAHGXMS than in DGXMS. This hypothesis, along with data measured for *p*-nitrophenyl β-D-Glc*p*A and reported[38] for methyl β-D-Glc*p*A (Table II, lines 2a, b), were used to make the chemical-shift assignments for the β-Glc*p*A substituents. The signal at 75.18 p.p.m. (Table II, line 2d) is assigned to C-2 of Glc*p*A in PAHGXMS (Fig. 2a); this is unambiguous on the basis of the relative-intensity changes observed.

Assignment of the anomeric-carbon signal of β-Glc*p*A in PAHGXMS is based on its relative intensity, its slight upfield shift on reduction (Table II, lines 2d and 3c), and J_{CH}. The coupling constant was estimated from the proton-coupled spectrum of PAHGXMS (not shown) to be 163 Hz. This value suggests that the signal is due to a β-anomeric carbon atom, probably of Glc*p*A. The corresponding J_{CH} values for the three most upfield anomeric signals for PAHGXMS (Fig. 2a) were definitively measured, and are appropriate for α-pyranoside units. Of these three signals (Table III, line 1b), the more upfield one, at 102.17 p.p.m. (J_{CH} 171 Hz), was tentatively assigned to C-1 of the α-Man*p* residue to which the β-Glc*p*A substituent is attached. The signal at 102.44 p.p.m. (J_{CH} 170 Hz) is due to C-1 of the α-Man*p* with 2-*O*-β-Xyl*p* attached as observed in XM (Table I, line 9a). The anomeric signal of lower intensity, at 103.29 p.p.m. (J_{CH} 174 Hz), is not assigned at this time (Fig. 2a). This signal is also present in the spectrum of DGXMS (Fig. 1c and Table III, line 1c). An analogous signal was observed at 103.86 p.p.m. in the spectrum of RGXMS, and at 103.80 p.p.m. in the spectrum of DRGXMS (Fig. 2b,c and Table III, lines 1d,f). If this signal were due to C-1 of β-Glc*p*A it would shift upfield on reduction to β-Glc*p* not downfield, as observed.

In addition to the chemical-shift assignment for C-1 of β-Glc*p* for RGXMS and DRGXMS, Table II (lines 3b,c) also contains tentative assignments for the other carbon atoms of the β-Glc*p* groups. These assignments are based on the spectral changes expected from comparison of the chemical shifts of the reference methyl and *p*-nitrophenyl glycosides, given in Table II (lines 2a,b and 3a), and upon the observed changes in the spectra (*cf.* GXMS *vs.* RGXMS, Figs. 1b and 2b, and especially DGXMS *vs.* DRGXMS, Figs. 1c and 2c). The most striking change observed was the disappearance of the C=O resonance at ~177 p.p.m. (not shown). In the spectra of the reduced polysaccharides the corresponding signal would coincide with the various other C-6 resonances of the Man*p* backbone residue at ~63 p.p.m. A change occurred for the C-4 resonance on reduction of GlcA. The

signal shifted upfield from ~74.2 p.p.m. for the nonreduced polysaccharides (Fig. 1b,c, 2a) to ~72.0 p.p.m. between the unchanged signals at 72.36 p.p.m. (Man*p* C-2) and 71.87 p.p.m. (Xyl*p* C-4) for RGXMS and DRGXMS (Fig. 2b,c). Reduction caused changes in the chemical shifts for the C-3 and C-5 resonances of Glc*p*A that resulted in an intense signal corresponding to the C-3 and C-5 resonances of Glc*p*. The separate absorptions at 77.94 and 79.21 p.p.m. for DGXMS (Fig. 1c) were replaced by the more intense broad signal at 78.65 p.p.m. for DRGXMS (Fig. 2c). Reduction caused a shift of the Glc*p*A C-2 resonance at 75.14 p.p.m. for DGXMS, and for DRGXMS the resonance appeared as an unresolved downfield shoulder on the β-Xyl*p* C-2 resonance at 75.37 p.p.m.

The signals in the spectral region of 60 to 108 p.p.m. (see Figs. 1 and 2) that are not already assigned to the resonances of β-Glc*p*A, β-Glc*p*, and β-Xyl*p* are probably due to the backbone α-Man*p*. The chemical shifts for these signals are given in Table III. Because no significant changes for the β-Xyl*p* and β-Glc*p* resonances were observed between the various polysaccharides, these units appear to be free from other attached substituents. The remaining lines in this region of the spectra of DGXMS and PAHGXMS, unassigned except as for XM, must be the result of glycosylation of Man*p* of the mannan backbone by the β-Glc*p*A groups.

If major substitutions occurred at O-6 or O-4 of the mannan, changes would be expected in the chemical shifts of the resonances for C-4, C-5, and C-6, but such changes were not observed, and thus, the β-Glc*p*A groups appear to be linked to neither O-6 nor O-4 of the mannan backbone. Therefore, these groups must be linked to O-2 atoms. Thus, the area of the nonsubstituted α-Man*p* C-2 resonances (72.3 p.p.m.) is diminished relative to the respective areas of C-4 and C-6 resonances in the spectra of DGXMS (Fig. 1c) and of PAHGXMS (Fig. 2a) when compared with those for XM (Fig. 1a). The related C-2 resonances are in the vicinity of 79 to 82 p.p.m., where several overlapping and poorly resolved signals are seen for DGXMS (Fig. 1c). Finally, the appearance of a second upfield anomeric carbon resonance at 102.2 p.p.m. (J_{CH} 171 Hz) for PAHGXMS and DGXMS, owing to an α-Man*p* residue, is also consistent with the conclusion that the α-Glc*p*A groups are attached to O-2 atoms of the mannopyranan backbone. If structures **2–5** are representative of XM, and if Glc*p*A residues are attached additionally to Man*p* O-2 sites in PAHGXMS and DGXMS, the question of whether they are connected to the Man*p*-a and/or Man*p*-b residues arises, but this question cannot be answered with the present data.

The location of the *O*-acetyl groups can be determined by comparison of the spectra of three pairs of polysaccharides, namely, those for GXMS and DGXMS (Fig. 1b,c), RGXMS and DRGXMS (Fig. 2b,c), and PM and DPM (Fig. 3a,b). Differences between the spectra of the first pair include: (*1*) the greatly lessened relative area of the Man*p* C-6 (~63.3 p.p.m.) and C-5 (~76.0 p.p.m.) signals for GXMS; (*2*) the presence of additional signals at 66.1 and 73.4 p.p.m. for GXMS (Fig. 1b and Table III, lines 5e and 6e)); and (*3*) the unresolved characteristics of the 80-p.p.m. spectral region for GXMS (Fig. 1b and Table III, line 3e). Parallels are

seen in the other pairs of spectra. The additional signals (point *2*) are prominent in the spectrum of PM (Fig. 3a and Table III, lines 5g, 6g) and, at a lower level, in that of RGXMS (Fig. 2b). On the basis of these data, the *O*-acetyl groups are linked at O-6 of Man*p*. This results in chemical-shift changes for C-6 and C-5 resonances of the *O*-acetylated Man*p* residues consistent with those reported[39] for 6-*O*-benzoylation of methyl α-D-Man*p*. The comparison between different acyl groups is reasonable in view of findings that a variety of acyl groups and solvents exhibit little difference in their influence on the changes in chemical shifts accompanying acylation of α- and β-D-Glc*p* species[40]. Both those mannan backbone residues that are 2-*O*-glycosylated and those that are not are 6-*O*-acetylated in about the same proportion, as deduced from the relative intensities of the two C-6 signals in the spectra of GXMS (63.64 and 63.22 p.p.m.) and DGXMS (63.72 and 63.20 p.p.m.) (Figs. 1b,c). On the basis of the relative areas of the two C-5 (75.97 and 73.41 p.p.m.) and of the three C-6 (66.12, 63.64, and 63.22 p.p.m.) signals in Fig. 1b, there is ~50% 6-*O*-acetylation of the Man*p* residues in GXMS. No other data in the spectra indicate any other sites of *O*-acetylation for GXMS, RGXMS, or PM, on either the mannan backbone or the side chains.

In summary, chemical methods have been employed for the generation of specified polysaccharide derivatives of GXM. Their ^{13}C-n.m.r. spectra have been used to make glycosidic linkage and configuration assignments and to determine the disposition of the side-chain groups. Molecular mechanics calculations have been used to estimate the difference among three minimal-energy conformations for the backbone mannan of GXM.

ACKNOWLEDGMENTS

The authors acknowledge support of this investigation by Public Health Service Grant AI 18877, and express their appreciation to Dr. M. E. Slodki of the Northern Regional Research Center, USDA, Peoria, Illinois, for helpful discussions.

REFERENCES

1. G. S. Bulmer and M. D. Sans, *J. Bacteriol.*, 94 (1967) 1475–1479.
2. G. S. Bulmer and M. D. Sans, *J. Bacteriol.*, 94 (1967) 1480–1483.
3. T. R. Kozel, *Infect. Immun.*, 16 (1977) 99–106.
4. T. R. Kozel and J. Cazin, Jr., *Infect. Immun.*, 3 (1971) 287–294.
5. R. A. Fromtling, H. J. Shadomy, and E. S. Jacobson, *Mycopathologia*, 79 (1982) 23–29.
6. A. K. Bhattacharjee, K. J. Kwon-Chung, and C. P. J. Glaudemans, *Immunochemistry*, 15 (1978) 673–679.
7. A. K. Bhattacharjee, K. J. Kwon-Chung, and C. P. J. Glaudemans, *Mol. Immunol.*, 16 (1979) 531–532.
8. A. K. Bhattacharjee, K. J. Kwon-Chung, and C. P. J. Glaudemans, *Carbohydr. Res.*, 73 (1979) 183–192.
9. A. K. Bhattacharjee, K. J. Kwon-Chung, and C. P. J. Glaudemans, *Carbohydr. Res.*, 82 (1980) 103–111.
10. R. Cherniak, E. Reiss, M. E. Slodki, R. D. Plattner, and S. O. Blumer, *Mol. Immunol.*, 17 (1980) 1025–1032.

11 E. H. MERRIFIELD AND A. M. STEPHEN, *Carbohydr. Res.*, 86 (1980) 69–76.
12 A. K. BHATTACHARJEE, K. J. KWON-CHUNG, AND C. P. J. GLAUDEMANS, *Carbohydr. Res.*, 95 (1981) 237–248.
13 D. E. WILSON, J. E. BENNETT, AND J. W. BAILEY, *Proc. Exp. Biol. Med.*, 127 (1968) 820–823.
14 R. IKEDA, A. NISHIKAWA, T. SHINODA, AND Y. FUKAZAWA, *Microbiol. Immunol.*, 29 (1985) 981–991.
15 A. K. BHATTACHARJEE, J. E. BENNETT, AND C. P. J. GLAUDEMANS, *Rev. Infect. Dis.*, 6 (1984) 619–624.
16 E. REISS, E. M. HUPPERT, AND R. CHERNIAK, *Curr. Top. Med. Mycol.*, 1 (1984) 172–207.
17 P. A. J. GORIN, *Adv. Carbohydr. Chem. Biochem.*, 38 (1981) 13–104.
18 R. CHERNIAK, E. REISS, AND S. H. TURNER, *Carbohydr. Res.*, 103 (1982) 239–250.
19 W. KAPLAN, S. L. BRAGG, S. CRANE, AND D. G. AHEARN, *J. Clin. Microbiol.*, 14 (1981) 313–317.
20 A. J. MORT AND W. D. BAUER, *J. Biol. Chem.*, (1982) 1870–1875.
21 A. J. MORT AND W. D. BAUER, *Plant Physiol.*, 66 (1980) 158–163.
22 I. J. GOLDSTEIN, G. W. HAY, B. A. LEWIS, AND F. SMITH, *Methods Carbohydr. Chem.*, 5 (1965) 361–370.
23 R. L. TAYLOR, J. E. SHIVELY, AND H. E. CONRAD, *Methods Carbohydr. Chem.*, 7 (1976) 149–151.
24 M. DUBOIS, K. A. GILLES, J. K. HAMILTON, P. A. REBERS, AND F. SMITH, *Anal. Chem.*, 28 (1956) 350–356.
25 N. BLUMENKRANTZ AND G. ASBOE-HANSEN, *Anal. Biochem.*, 54 (1973) 484–489.
26 S. H. TURNER AND R. CHERNIAK, *Carbohydr. Res.*, 95 (1981) 137–144.
27 C. HARA, T. KIHO, AND S. UKAI, *Carbohydr. Res.*, 111 (1982) 143–150.
28 P. A. J. GORIN, *Can. J. Chem.*, 51 (1973) 2375–2383.
29 P. A. J. GORIN, *Carbohydr. Res.*, 39 (1975) 3–10.
30 A. ALLERHAND AND E. BERMAN, *J. Am. Chem. Soc.*, 106 (1984) 2400–2412.
31 F. KONG AND C. SCHUERCH, *Macromolecules*, 17 (1984) 983–989.
32 D. A. REES, E. R. MORRIS, D. THOM, AND J. K. MADDEN, in G. O. ASPINALL (Ed.), *The Polysaccharides*, Vol. 1, Academic Press, New York, 1982, pp. 195–290.
33 K. OGAWA, T. MIYANISHI, T. YUI, C. HARA, T. KIHO, S. UKAI, AND A. SARKO, *Carbohydr. Res.*, 148 (1986) 115–120.
34 V. WARIN, F. BAERT, R. FOURET, G. STRECKER, G. SPIK, B. FOURNET, AND J. MONTREUIL, *Carbohydr. Res.*, 76 (1979) 11–22.
35 J. R. BRISSON AND J. P. CARVER, *Biochemistry*, 22 (1983) 1362–1368.
36 U. BURKERT AND N. L. ALLINGER, *Molecular Mechanics, ACS Monograph* 177, American Chemical Society, Washington, D. C., 1982.
37 G. H. FLEET, *Curr. Top. Med. Mycol.*, 1 (1984) 23–56.
38 P. A. J. GORIN AND M. MAZUREK, *Can. J. Chem.*, 53 (1975) 1212–1223.
39 Y. TSUDA, M. E. HAQUE, AND K. YOSHIMOTO, *Chem. Pharm. Bull.*, 31 (1983) 1612–1624.
40 K. YOSHIMOTO, Y. ITATANI, AND T. TSUDA, *Chem. Pharm. Bull.*, 28 (1980) 2065–2076.
41 K. BOCK AND C. PEDERSEN, *Adv. Carbohydr. Chem. Biochem.*, 41 (1983) 27–66.